Casimir effect between superconductors

Giuseppe Bimonte*
Dipartimento di Fisica E. Pancini, Università di Napoli Federico II, Complesso Universitario di Monte S. Angelo, Via Cintia, I-80126 Napoli, Italy
and INFN Sezione di Napoli, I-80126 Napoli, Italy

(Received 25 February 2019; published 14 May 2019)

A recent experiment [Norte *et al.* Phys. Rev. Lett. **121**, 030405 (2018)] probed the variation of the Casimir force between two closely spaced thin Al films as they transition into a superconducting state, observing a null result. We present here computations of the Casimir effect for superconductors, based on the Mattis-Bardeen formula for their optical response. We show that for the Al system used in the experiment the effect of the transition is over 250 times smaller than the experimental sensitivity, in agreement with the observed null result. We demonstrate that a large enhancement of the effect can be achieved by using a system consisting of a Au mirror and a superconducting NbTiN film. We estimate that the effect of the superconducting transition would be observable with the proposed Au-NbTiN configuration, if the sensitivity of the apparatus could be increased by an order of magnitude.

DOI: 10.1103/PhysRevA.99.052507

I. INTRODUCTION

One of the most spectacular manifestations of vacuum fluctuations of quantum fields is provided by the Casimir effect [1]. This is the tiny force acting between two discharged dielectric bodies, which results from the modification of the spectrum of quantum and thermal fluctuations of the electromagnetic field in the region of space bounded by the two bodies. In his pioneering work, Casimir studied this phenomenon for the idealized case of two perfectly conducting plane-parallel mirrors at zero temperature. The investigation of the Casimir effect in real material media started with the fundamental paper of Lifshitz [2], which presented a derivation of the force between two plane-parallel dielectric slabs in vacuum, at finite temperature. In recent years, intense experimental and theoretical efforts have been made to probe the dependence of the Casimir force on the shapes and material properties of the test bodies. For a review of the Casimir effect, and its perspective applications to nanotechnology the reader may consult several recent books and review articles [3–10].

Many experiments have now probed the Casimir effect with test bodies made of diverse materials, embedded in different media. Apart from two metallic conductors in vacuum, which still constitute the standard configuration, experiments have been carried out with semiconductors [11–13], conductive oxides [14–16], magnetic materials [17,18], and liquid crystals [19]. Experiments exist as well in which the bodies are immersed in gases or in liquids [20,21].

Another interesting class of candidate materials for Casimir experiments is represented by superconductors [22,23]. The study of the Casimir effect in superconductors is indeed very interesting, since these materials constitute an excellent arena [24] to investigate yet unresolved fundamental problems [5,6] about the influence of relaxation phenomena on the strength of the Casimir force between metallic bodies. Unfortunately, observing the influence of the superconducting transition on the Casimir effect is very difficult, because on theory grounds one expects that the effect is extremely small. This can be understood by considering that the transition modifies significantly the optical properties of a superconductor only for frequencies of the order of $k_B T_c/\hbar$, where T_c is the critical temperature. This region represents only a very small fraction of the spectrum of frequencies that contribute to the Casimir interaction between two bodies at distance a. The latter spectrum is known to stretch up to the characteristic frequency $\omega_c = c/a$, which for typical sub-μm separations is tens of thousands times larger than the frequency $k_B T_c/\hbar$ for classical BCS superconductors. In view of the difficulty of a direct force measurement, in Refs. [22,23] we proposed an indirect approach, based on observation of the Casimir-induced shift of the critical magnetic field H_c of a thin superconducting film, constituting one of the two plates of a rigid Casimir apparatus. An experiment with an Al film based on this scheme, placed an upper bound on the shift of the critical field not far from theoretical predictions [25,26].

An alternative route to successful detection is represented by differential measurements, which offer the advantage of a far superior sensitivity in comparison to absolute force measurements. An experiment based on the observation of the differential Casimir force between a Au-coated sphere and the two sectors of a microfabricated plate, respectively, made of superconducting Nb and Au, was indeed proposed in Ref. [27]. The latter setup exploits the principle of isoelectronic differential measurements [28,29], whose power in precision Casimir measurements has been demonstrated by a room temperature experiment [18] with a microfabricated plate consisting of alternating Au and Ni sectors.

More recently, an unpublished experiment [30] measured the Casimir force between a Au-coated sphere with a

*giuseppe.bimonte@na.infn.it

radius $R = 100\ \mu$m and a superconducting NbTiN film, with a critical temperature $T_c = 13.6$ K. The experimental data for room temperature showed good agreement with theoretical predictions. The low-temperature data displayed, however, an anomalous behavior, due to an unexpected 20% increase in the measured force, for which no explanation could be found. Apart from this, the experiment did not detect any change in the strength of the Casimir force across the superconducting transition, and placed an upper bound of 2.6% on the maximum magnitude of the ensuing variation of the Casimir force.

A promising on-chip platform for observing the Casimir force between superconductors has been described very recently in Ref. [31]. The apparatus consists of two microfabricated Al-coated SiN parallel strings, having a length of $384\,\mu$m and a width of 926 nm. By application of a large tensile stress, the strings can be kept perfectly parallel, at litographically determined fixed separations. Several cavities of different widths were realized on the same chip, the minimum separation being of one hundred nm. One of the two strings is attached to the movable mirror of an optomechanical cavity, whose resonance frequency is monitored by a laser. The detection scheme is based on the idea that when the system transitions to superconductivity, the resulting variation of the Casimir force between the Al strings should affect the mutual distance between the strings, thus determining a change in the length of the cavity and therefore in its resonance frequency. The experiment [31] provides a nice implementation the differential measurement scheme, since the apparatus is sensitive to the variation $\Delta F(T) = F(T) - F(T_c)$ across the superconducting transition of the Casimir force $F(T)$ on the Al strings. Up to edge effects, the force $F(T)$ can be expressed as $F(T) = P(T) \times A$, where $P(T)$ is the unit-area Casimir force, i.e., the Casimir pressure, and A is the area of the strings. The above relation shows that the measurement of $\Delta F(T)$ is directly related to the variation $\Delta P(T) = P(T) - P(T_c)$ of the Casimir pressure across the critical temperature of the superconducting transition ($T_c = 1.2$ K for Al). The null result reported by the experiment sets on the magnitude of ΔP an upper bound of 6 mPa, which represents the sensitivity of the apparatus.

In this paper we work out a detailed theory of the Casimir effect between superconductors. We compute the variation $\Delta P(T)$ of the Casimir pressure for two distinct configurations of a superconducting plane-parallel system. In the first configuration, similarly to the experiment [31], both plates are made of the same superconductor, while in the second configuration, similarly to the experiment [30], one of the two superconducting plates is replaced by a Au mirror. We model the frequency-dependent permittivity of the superconductor by the Mattis-Bardeen formula [32,33], which provides the best known description of the optical properties of superconductors. We present numerical results for NbTiN and Al, which are the superconductors used in the experiments [30] and [31], respectively. It is important to note that optical measurements performed on NbTiN superconducting films [34] show excellent agreement with the local limit (so called dirty limit) of the Mattis-Bardeen formula, providing strong support in favor of our theoretical model. Our computations show that for the Al setup used in the experiment [31] the magnitude of ΔP is over 250 times smaller than the experimental sensitivity. Our results, while in agreement with the null result reported by the experiment, make it unlikely that the effect of the superconducting transition can be observed with an Al system. We find, however, that the magnitude of $\Delta P(T)$ can be enhanced by a factor of 15, by considering a setup composed by a Au mirror and a NbTiN film, having a thickness larger than 200 nm. The enhancement factor increases to 34 if the separation a is decreased from 100 nm to 60 nm. This is an encouraging result, since it shows that the effect would be detectable with a Au-NbTiN setup, if the sensitivity of the apparatus could be improved by one order of magnitude.

The plan of the paper is as follows. In Sec. II we review the general formalism for computing the Casimir pressure between two superconducting parallel plates, and we present the models we use to describe their optical properties. In Sec. III we present the results of our numerical computations. In Sec. IV we present our conclusions. Finally, in the Appendix we provide the explicit formula for the analytic continuation to the imaginary frequency axis of the Mattis-Bardeen formula for the frequency-dependent conductivity of BCS superconductors.

II. GENERAL FORMALISM FOR THE CASIMIR PRESSURE

We consider a Casimir setup, formed by two plane-parallel homogeneous and isotropic dielectric plates at temperature T, separated by an empty gap of width a. We denote by $\epsilon^{(k)}(\omega)$, $k = 1, 2$ their respective (complex) permittivities (we only consider nonmagnetic materials, and thus we set $\mu^{(1)} = \mu^{(2)} \equiv 1$). According to Lifshitz formula [2], the Casimir pressure $P(a, T)$ among the plates can be expressed as (negative pressures correspond to attraction):

$$P(a,T) = -\frac{k_B T}{\pi} {\sum_{l=0}^{\infty}}' \int_0^\infty dk_\perp k_\perp q_l \times \sum_\alpha \left[\frac{e^{2aq_l}}{r_\alpha^{(1)}(i\xi_l, k_\perp) r_\alpha^{(2)}(i\xi_l, k_\perp)} - 1 \right]^{-1}, \quad (1)$$

where k_B is Boltzmann constant, $k_\perp$ is the in-plane momentum, the prime in the sum indicates that the $l = 0$ term is taken with weight one-half, $\xi_l = 2\pi l k_B T/\hbar$ are the imaginary Matsubara frequencies, $q_l = \sqrt{\xi_l^2/c^2 + k_\perp^2}$, and the sum over $\alpha =$ TE, TM is taken over the independent states of polarization of the electromagnetic field, i.e., transverse magnetic (TM) and transverse electric (TE). Finally, the symbols $r_\alpha^{(k)}(i\xi_l, k_\perp)$ denote the Fresnel reflection coefficients of the kth slab:

$$r_{\rm TE}^{(k)}(i\xi_l, k_\perp) = \frac{q_l - s_l^{(k)}}{q_l + s_l^{(k)}}, \quad (2)$$

$$r_{\rm TM}^{(k)}(i\xi_l, k_\perp) = \frac{\epsilon_l^{(k)} q_l - s_l^{(k)}}{\epsilon_l^{(k)} q_l + s_l^{(k)}}, \quad (3)$$

where $s_l^{(k)} = \sqrt{\epsilon_l^{(k)} \xi_l^2/c^2 + k_\perp^2}$, and $\epsilon_l^{(k)} \equiv \epsilon^{(k)}(i\xi_l)$. If instead of thick homogeneous slabs, one considers more complex mirrors constituted by plane-parallel metallic films deposited on some substrate, the corresponding Casimir pressure can

still be computed by the general Lifshitz formula Eq. (1), provided that the Fresnel reflection coefficients Eqs. (2)–(3) are replaced by the reflection coefficients of the layered mirrors [5]. We will consider two distinct configurations for our system: in the first one, both plates are made of the same superconducting material. Concretely, we will consider two superconductors, i.e., Al (which is the superconductor used in the experiment [31]), and NbTiN (which is the superconductor used in the experiment [30]). The corresponding configurations will be denoted as Al-Al and NbTiN-NbTiN, respectively. The respective Casimir pressures are obtained by substituting into Lifshitz formula the permittivities of Al or NbTiN, respectively: $\epsilon_l^{(1)} = \epsilon_l^{(2)} = \epsilon^{(\mathrm{Al/NbTiN})}(i\xi_l)$. In the second configuration, one of the two superconducting plates is replaced by a Au mirror. This second configuration will be analyzed in detail only for the case of NbTiN, and we will denote it as the Au-NbTiN configuration. The corresponding Casimir pressure is obtained by setting into Eq. (1) $\epsilon_l^{(1)} = \epsilon^{(\mathrm{Au})}(i\xi_l)$ and $\epsilon_l^{(2)} = \epsilon^{(\mathrm{NbTiN})}(i\xi_l)$.

To compute the Casimir pressure, one needs the permittivities $\epsilon_l^{(k)}$ of the materials constituting the plates. In a concrete experimental situation, one would ideally like to measure the optical data of the used samples, for the experimental values of the temperature. The permittivities $\epsilon_l^{(k)}$ for the physically inaccessible imaginary frequencies $i\xi_l$ would then be computed on the basis of the optical data, using Kramers-Kronig dispersion relations [5]. In order to obtain a precise theoretical estimate of the Casimir pressure $P(a, T)$ for a separation a, it is in principle necessary to know the optical data for all frequencies lower than ten or twenty times the characteristic frequency $\omega_c = c/2a$ [5]. For $a = 100$ nm, $\omega_c = 1.5 \times 10^{15}$ rad/s.

It is fortunate that in the problem at hand we do not really need this much information about the optical properties of the materials. Indeed, the quantity that interests us is not the Casimir pressure $P(a, T)$ at a single temperature, but rather its variation $\Delta P(a; T)$ across the critical temperature T_c:

$$\Delta P(a; T) = P(a, T) - P(a, T_c), \tag{4}$$

where $T < T_c$. Now, it is known [33] that the superconductive transition affects significantly the optical properties of a superconductor only for frequencies corresponding to photon energies smaller than (a few times) the BCS gap $\Delta(0)$. From BCS theory [33] one knows that $\Delta(0) = 1.76 k_B T_c$. For Al ($T_c = 1.2$ K) this gives $\Delta(0) = 1.8 \times 10^{-4}$ eV, while for NbTiN ($T_c = 13.6$ K) $\Delta(0) = 2.1 \times 10^{-3}$ eV. For these small photon energies the optical response of a normal metal is dominated by intraband transitions. The latter can be phenomenologically described by a Drude-model dielectric function of the form

$$\epsilon(i\xi) = \epsilon_0 + \frac{\Omega^2}{\xi(\xi + \gamma)}, \tag{5}$$

where the contribution from core interband transitions has been included in ϵ_0. Here Ω is the plasma frequency for intraband transitions, and γ is the relaxation frequency. To compute ΔP we have used the simple Drude model in Eq. (5) to describe the permittivity of Au, as well as the permittivity of the superconductors in the normal state. In our computations we have neglected the temperature dependence of both the plasma frequency Ω and of the core-electron permittivity ϵ_0, and thus we used their room-temperature values. The relaxation frequency is instead temperature dependent, and in general it decreases as the temperature is decreased. At cryogenic temperatures γ approaches a constant sample-dependent residual value. Following the standard convention, we express the residual relaxation frequency in terms of the corresponding room-temperature frequency γ_0 by the formula $\gamma = \gamma_0/\mathrm{RRR}$ where RRR is the residual resistance ratio. The values of the parameters were chosen as follows. For Au, we used the standard values $\Omega = 9$ eV$/\hbar$ and $\gamma_0 = 35$ meV$/\hbar$ [5], while from the tabulated optical data [35] we obtained $\epsilon_0 = 6.3$. For Al, we used $\Omega = 13$ eV$/\hbar$, $\gamma_0 = 100$ meV$/\hbar$, and $\epsilon_0 = 1.03$ [35]. Finally, for NbTiN we used the values quoted in Ref. [30], i.e., $\Omega = 5.33$ eV$/\hbar$ and $\gamma_0 = 0.465$ eV$/\hbar$. In Ref. [30] the optical data of the used NbTiN films were determined by ellipsometry in the frequency range from 1.89×10^{11} rad/s to 1.13×10^{16} rad/s, both at room temperature and at 16 K. The optical data were afterwards fitted by a Lorentz-Drude model with four oscillator terms. Unfortunately the values of the corresponding parameters were not reported explicitly. We are thus unable to provide a value for the contribution of core electrons for this material. We have verified however that the pressure variation $\Delta P(a; T)$ remains practically unchanged when the value ϵ_0 for NbTiN is varied in the interval from one to ten. The value of the RRR parameter depends on the sample preparation procedure, and therefore it cannot be fixed *a priori*. For the NbTiN sample used in the experiment [30], the fit to the optical data at 16 K gave $\gamma = 0.415$, which corresponds to RRR $= 1.12$. To probe the sensitivity of the pressure variation ΔP on this parameter, in our computations we varied its value in the interval from one to ten.

Next, we describe the model for the permittivity of the superconductors. For this we rely on the Mattis-Bardeen formula [32] for the conductivity σ, which is known to provide an accurate representation of the optical response of BCS superconductors [33]. In its general form, the Mattis-Bardeen formula depends both on the frequency ω and the wave vector q, since superconductors display spatial dispersion. However, the q dependence is negligible in the so-called dirty limit $\ell/\xi_0 \ll 1$, where $\ell = v_F/\gamma$ is the mean free path, and $\xi_0 = \hbar v_F/\pi\Delta(0)$ is the correlation length, with v_F the Fermi velocity. The dirty limit condition is well satisfied by both Al ($\ell/\xi_0 = 5.7 \times 10^{-3}$) and NbTiN ($\ell/\xi_0 = 1.4 \times 10^{-2}$). This is confirmed by optical measurements of NbTiN films in the THz region, that are in excellent agreement with the local dirty limit of the Mattis-Bardeen formula [34]. The analytic continuation of the Mattis-Bardeen formula to the imaginary frequency axis has been worked out in Ref. [37], where it is shown that $\sigma_{\mathrm{BCS}}(i\xi)$ can be conveniently decomposed as:

$$\sigma_{\mathrm{BCS}}(i\xi) = \frac{\Omega^2}{4\pi}\left[\frac{1}{(\xi + \gamma)} + \frac{g(\xi; T)}{\xi}\right], \tag{6}$$

The first term between the square brackets on the right-hand side (r.h.s.) of the above Equation coincides with the familiar Drude contribution to the conductivity of a normal metal, while the second term represents the BCS correction. The explicit expression of the function $g(\xi)$ is given in the Appendix.

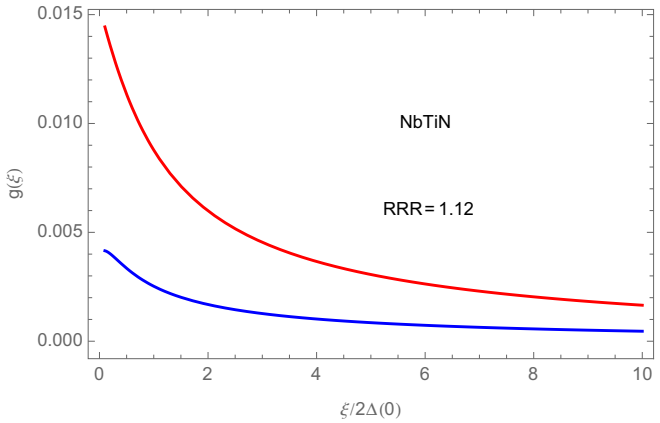

FIG. 1. Plot of $g(\xi)$ [see Eq. (6)] for NbTiN (RRR = 1.12), versus $\xi/2\Delta(0)$ for $T/T_c = 0.9$ (lower blue line), and $T/T_c = 0.1$ (upper red line).

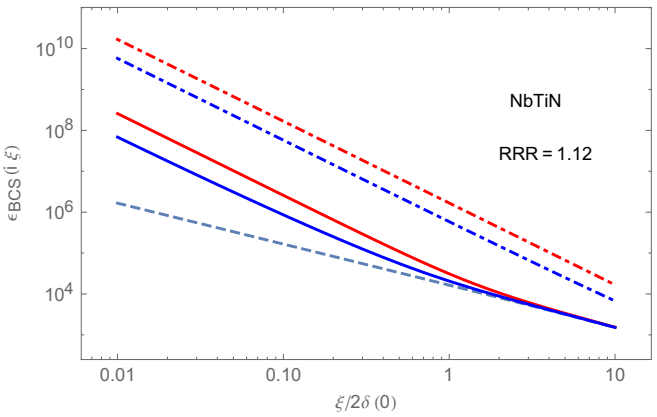

FIG. 2. BCS permittivity of NbTiN (RRR = 1.12) versus $\xi/2\Delta(0)$ for $T/T_c = 0.9$ (solid blue line) and $T/T_c = 0.1$ (solid red line). The dashed line shows the Drude permittivity Eq. (5). The dot-dashed lines show the permittivity for the Casimir-Gorter two-fluid model, for $T/T_c = 0.9$ (dot-dashed blue line), and $T/T_c = 0.1$ (dot-dashed red line)

Here is a brief summary of its main properties. The function $g(\xi)$ is different from zero only for $T < T_c$, and vanishes identically for $T \to T_c$. For $T < T_c$, it is a positive and monotonically decreasing function of $\xi > 0$, approaching a finite value $g(0) < 1$ for $\xi \to 0$, and going to zero for $\xi \to \infty$. Its value depends parametrically on the temperature-dependent BCS gap $\Delta(T)$ as well as on the relaxation frequency γ. In addition to that, $g(\xi)$ has an explicit dependence on the temperature. For small ξ the function $g(\xi)$ has the expansion:

$$g(\xi;T) = \omega_s^2(T) + B(T)\xi\log(\Delta/\hbar\xi) + o(\xi), \qquad (7)$$

where $\omega_s(T)$ represents the (normalized) effective superfluid plasma frequency. A plot of the function $g(\xi;T)$ for NbTiN (RRR = 1.12) is shown in Fig. 1 for $T/T_c = 0.9$ (blue line) and for $T/T_c = 0.1$ (red line). By adding the contribution of core electrons, we thus arrive at the following formula for the permittivity of the superconductor:

$$\epsilon_{BCS}(i\xi) = \epsilon_0 + 4\pi\frac{\sigma_{BCS}(i\xi)}{\xi} = \epsilon_0 + \frac{\Omega^2}{\xi}\left[\frac{1}{\xi+\gamma} + \frac{g(\xi;T)}{\xi}\right]. \qquad (8)$$

The BCS term proportional to $g(\xi;T)$ in the expression of ϵ_{BCS} can be interpreted as a plasma-model contribution, with an effective ξ-dependent plasma frequency $\Omega_{\rm eff}(\xi) = \Omega\sqrt{g(\xi;T)}$. In Fig. 2 we show logarithmic plots of the BCS permittivity of NbTiN as a function of $\xi/2\Delta(0)$, for $T/T_c = 0.9$ (blue line) and for $T/T_c = 0.1$ (red line). The dashed line corresponds to the Drude permittivity Eq. (5). The figure shows that the BCS permittivity approaches the Drude permittivity for $\xi/2\Delta(0) \gg 1$.

It is interesting to compare the BCS formula for the permittivity with the old-fashioned Casimir-Gorter two-fluid model [33,36]. According to this model a fraction $n_s(T)$ of the conduction electrons contributes to the supercurrent, while the remaining fraction $n_n(T) = 1 - n_s(T)$ remains normal. Superconducting electrons behave as a dissipationless plasma, while normal electrons are described by the usual dissipative Drude model. Core electron remain unaltered. According to this simple physical picture, the permittivity of the two-fluid model is written as:

$$\epsilon(i\xi) = \epsilon_0 + (1 - n_s(T))\frac{\Omega^2}{\xi(\xi+\gamma)} + n_s(T)\frac{\Omega^2}{\xi^2}. \qquad (9)$$

The fraction $n_s(T)$ of superconducting electrons follows the Casimir-Gorter law:

$$n_s(T) = \left[1 - \left(\frac{T}{T_c}\right)^4\right]\Theta(T_c - T), \qquad (10)$$

where $\Theta(x)$ is the Heaviside step function: $\Theta(x) = 1$ for $x > 0$, and $\Theta(x) = 0$ for $x \leqslant 0$. In Fig. 2 we show plots of the two-fluid model for NbTiN, for $T/T_c = 0.9$ (blue dot-dashed line) and for $T/T_c = 0.1$ (red dot-dashed line). Comparison with the BCS permittivity (solid lines) shows that the two-fluid model overestimates the permittivity of a superconductor by a very large factor. We note that the two fluid model was used in Ref. [30] to compute the Casimir force between superconductors.

III. NUMERICAL COMPUTATION OF ΔP

In this section we present our numerical computations of the pressure variation $\Delta P(a;T)$, based on the expressions of the permittivity described in the previous section. In particular, for the permittivity of the superconductors we use the BCS formula Eq. (8), where the function $g(\xi;T)$ has the expression provided in the Appendix.

We consider first a Casimir setup constituted by two thick plates made of Al, which is the superconductor used in the experiment [31]. In Fig. 3 the corresponding $\Delta P(a;T)$ is plotted versus the temperature T (in K), for the separation $a = 100$ nm, which was the minimum separation probed in the experiment. We took RRR = 1. For comparison, we show in the same figure the variation of the pressure that would obtain in the absence of the transition (dashed line). We see that the solid curve lies below the dashed one, in accordance with one's expectation that the superconducting transition determines an increase in the Casimir attraction with respect

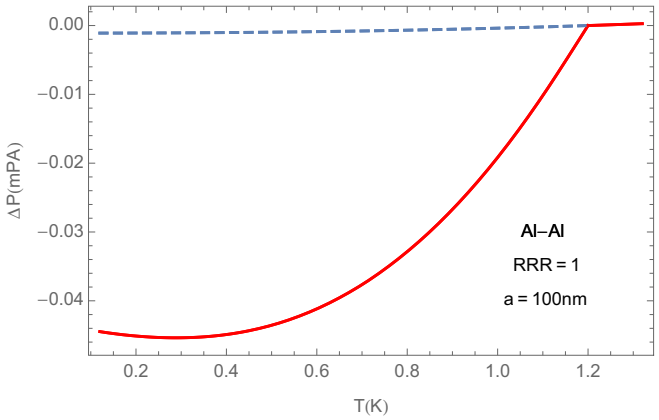

FIG. 3. Variation of the Casimir pressure across the superconducting transition of an Al plane-parallel system with thick walls, versus temperature (in K). The dashed line represents the variation of the Casimir pressure in the absence of the transition.

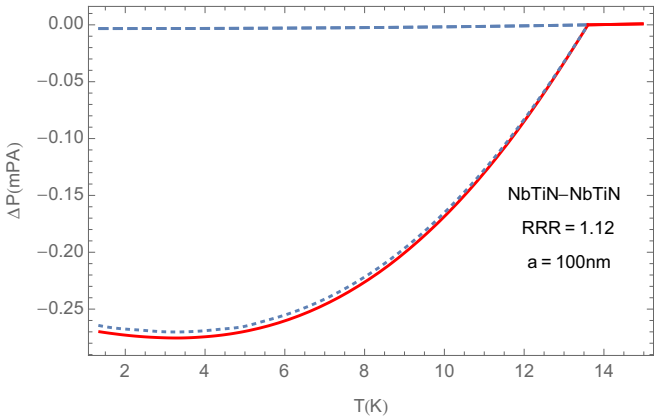

FIG. 5. Variation of the Casimir pressure across the superconducting transition of a NbTiN plane-parallel setup, versus temperature (in K). The dashed line represents the variation of the Casimir pressure in the absence of the transition. The solid and dotted lines correspond, respectively, to taking $\epsilon_0 = 1$ and $\epsilon_0 = 10$ in the permittivity of NbTiN [see Eq. (5)].

to the normal state, since superconductors are better reflectors than normal metals. The magnitude of ΔP is seen to be smaller than 0.05 mPa at all temperatures below T_c. To get a feeling of how small an effect this represents, we note that the magnitude of the Casimir force $P(T_c)$ at the critical temperature is estimated to be of 6.8 Pa [this value was computed using the simple representation Eq. (5) for the permittivity of Al, and must be just considered as an approximate estimate. A more accurate estimate would require a better description of core electrons]. Using this estimate, we obtain $\Delta P/P(T_c) < 7 \times 10^{-6}$ across the transition.

The Casimir setup used the experiment [31] consisted of two identical layered plates, each consisting of an Al film with a thickness $w = 18$ nm, deposited on a SiN substrate. To determine how the thickness w of the Al films influences ΔP, it is necessary to replace in Lifshitz formula the Fresnel reflection coefficients for a thick Al slab Eqs. (2)–(3) by those for the layered Al-SiN plate [5]. The results of this computation are shown in Fig. 4 (we took $\epsilon_0 = 4$ for the dielectric constant of SiN). We see that the thick-plate limiting

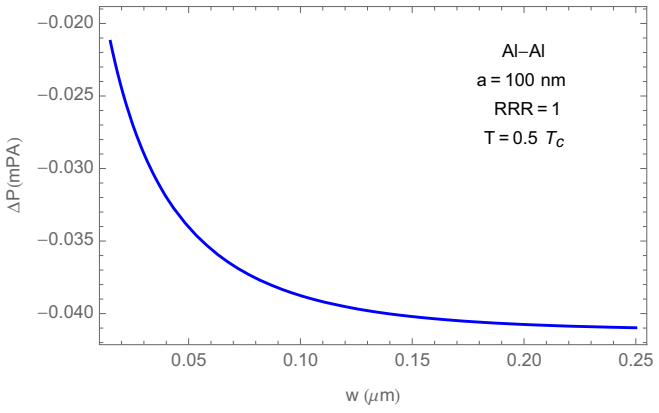

FIG. 4. Variation of the Casimir pressure across the superconducting transition of an Al system consisting of two identical Al films of thickness w deposited on a SiN substrate, versus films thickness w (in μm).

value of 0.041 mPa is nearly reached for a film thickness of 250 nm, but for a thickness of 18 nm the magnitude of ΔP decreases to 0.023 mPa. Recalling that the experiment [31] has an estimated sensitivity of 6 mPa, we see that the theoretical pressure variation for the Al setup is over 250 times smaller than the sensitivity. While this is consistent with the null result reported by the experiment, it makes one think that observation of the effect with the Al system is hardly possible in the near future.

Our computations predict that a significant increase in the magnitude of the pressure variation can be achieved by using NbTiN in the place of Al. This is demonstrated by Fig. 5, which displays the pressure variation for two thick NbTiN plates at a separation $a = 100$ nm, versus the temperature T (RRR = 1.12). As we said earlier, we could not find in the literature enough information on the optical properties of NbTiN, to fix the value of ϵ_0 in Eq. (8). For this reason, we repeated the computations using two widely different values for ϵ_0. It is fortunate that the pressure variation is insensitive to the contribution of core electrons, as it can be seen from Fig. 5 where the solid and dotted lines correspond to $\epsilon_0 = 1$ and $\epsilon_0 = 10$, respectively. The weak dependence of ΔP on ϵ_0 is explained by the fact that the pressure variation is determined by the optical response of the materials at frequencies of the order the thermal frequency $k_B T_c/\hbar$, for which the Drude term is overwhelmingly large compared to ϵ_0. Comparison of Fig. 5 with Fig. 3 shows that the variation of the Casimir pressure for a NbTiN setup is five times larger than the corresponding variation for an Al system.

A further increase of the pressure variation can be achieved by replacing one of the NbTiN plates by a Au mirror. This is so because Au is a better reflector than NbTiN, due to its larger plasma frequency (recall that $\Omega_{\rm Au} = 9$ eV$/\hbar$, while $\Omega_{\rm NbTiN} = 5.33$ eV$/\hbar$). We note that Au-NbTiN was the combination of materials adopted in the unpublished experiment [30]. We assume in what follows that the thickness of the Au coating of the first mirror is larger than 200 nm. This ensures that for the purposes of the Casimir effect that mirror can be considered

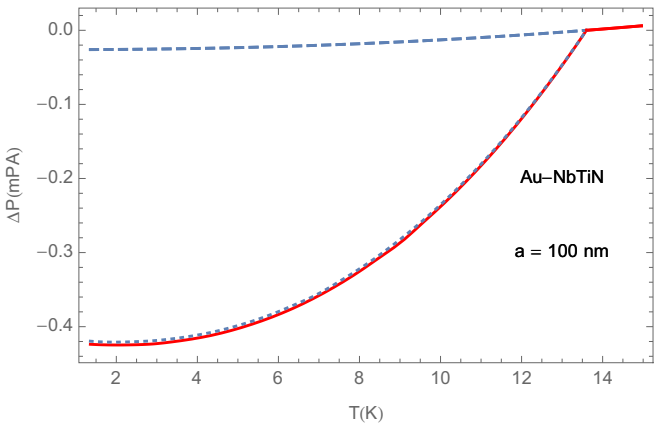

FIG. 6. Variation of the Casimir pressure across the superconducting transition of a Au-NbTiN plane-parallel system, versus temperature (in K). The dashed line represents the variation of the Casimir pressure in the absence of the transition. The solid and dotted lines correspond, respectively, to taking $\epsilon_0 = 1$ and $\epsilon_0 = 10$ in the permittivity of NbTiN [see Eq. (5)]. Data are for $\mathrm{RRR}_{\mathrm{NbTiN}} = 1.12$ and $\mathrm{RRR}_{\mathrm{Au}} = 1$.

as equivalent to an infinitely thick Au slab [5]. We note that Ref. [30] does not provide data for the RRR of Au at 16 K. In our computations we take $\mathrm{RRR}_{\mathrm{Au}} = 1$. It can be seen from Fig. 6 that for $a = 100$ nm the maximum variation pressure for the Au-NbTiN system has a magnitude of 0.42 mPa, which is nine times larger than the corresponding maximum pressure variation of the Al system (see Fig. 3). In Fig. 7 we show the pressure variation of the Au-NbTiN setup as a function of the separation a (in nm), for $T/T_c = 0.5$. The red and blue curves correspond to $\mathrm{RRR}_{\mathrm{NbTiN}} = 1.12$ and $\mathrm{RRR}_{\mathrm{NbTiN}} = 5$, respectively. In Fig. 8 the pressure variation is displayed versus the residual resistance ratio RRR of the NbTiN film, for the two separations $a = 100$ nm (upper red curve) and $a = 60$ nm (lower blue curve). In Fig. 9 the pressure variation is displayed versus the residual resistance ratio RRR of the Au film, for the two separations $a = 100$ nm (upper red curve)

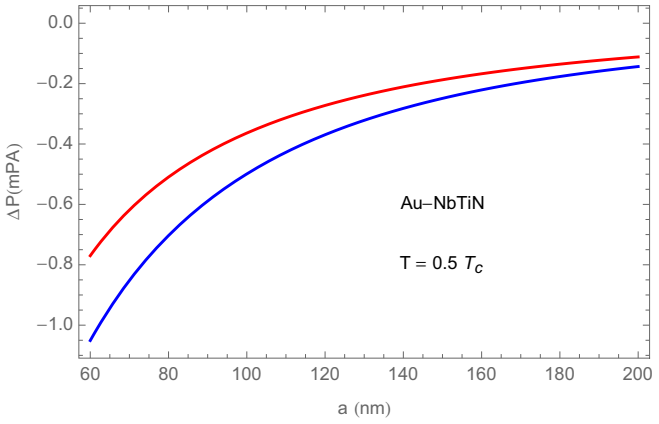

FIG. 7. Variation of the Casimir pressure across the superconducting transition of a Au-NbTiN plane-parallel system, versus separation a (in nm). The upper red line and the lower blue line correspond, respectively, to residual resistance ratios RRR = 1.12 and RRR = 5 for the NbTiN film. In both cases $\mathrm{RRR}_{\mathrm{Au}} = 1$.

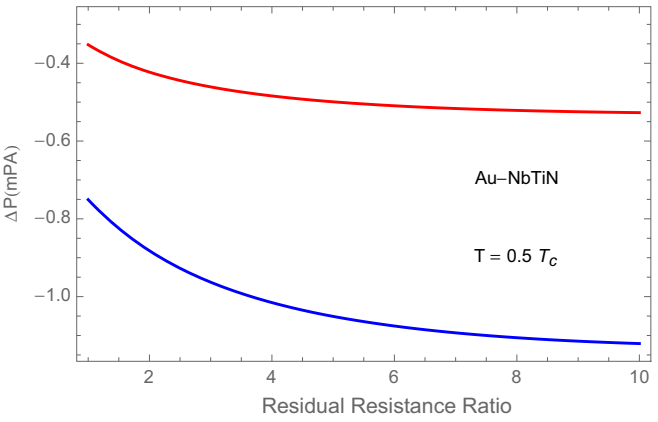

FIG. 8. Variation of the Casimir pressure across the superconducting transition of a Au-NbTiN plane-parallel system, versus the RRR of the NbTiN plate. The RRR of the Au plate is fixed to one. The upper red line and the lower blue line correspond respectively to the separations $a = 100$ nm and $a = 60$ nm.

and $a = 60$ nm (lower blue curve). For both curves, the RRR of the NbTiN film has the fixed value $\mathrm{RRR}_{\mathrm{NbTiN}} = 1.12$. We note that by increasing the value of RRR for the Au plate, it is possible to obtain a significant increase in the magnitude of ΔP. This indicates that it would be beneficial to realize a Au mirror having a long mean free path for the electrons. Finally, in Fig. 10 we display the pressure variation of the system formed by a thick Au mirror and a NbTiN film of thickness w, as a function of the film thickness w (in μm), for a fixed separation $a = 100$ nm. The pressure variation is moderately dependent on the properties of the substrate of the superconducting film. We verified this by comparing the results for a freestanding film (solid line of Fig. 10) with those for a substrate having a static permittivity equal to 10 (dashed line in Fig. 10). The influence of the substrate of course decreases for thicker films. The plot shows that NbTiN films with a thickness larger than 200 nm are essentially undistinguishable from an infinitely thick slab.

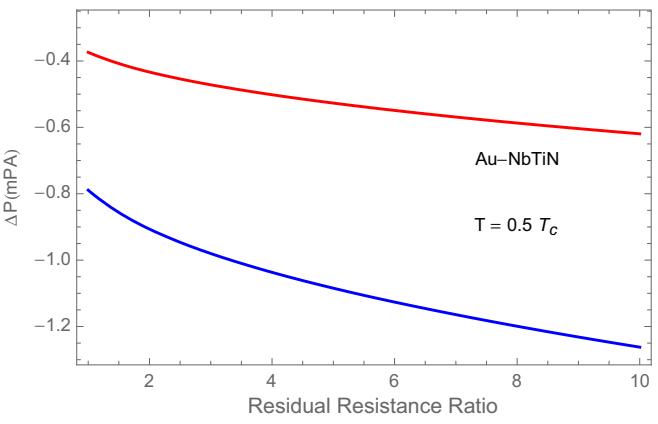

FIG. 9. Variation of the Casimir pressure across the superconducting transition of a Au-NbTiN plane-parallel system, versus the RRR of the Au plate. The RRR of the NbTiN plate is fixed to RRR = 1.12. The upper red line and the lower blue line correspond respectively to the separations $a = 100$ nm and $a = 60$ nm.

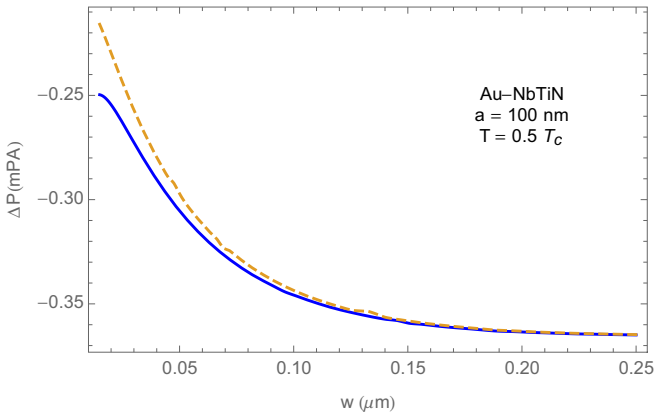

FIG. 10. Variation of the Casimir pressure across the superconducting transition of a plane-parallel system formed by a thick Au mirror and a NbTiN film of thickness w, versus film thickness w in μm. Shown data are for $\mathrm{RRR}_{\mathrm{NbTiN}} = 1.12$ and $\mathrm{RRR}_{\mathrm{Au}} = 1$. The solid and dashed lines correspond, respectively, to a freestanding NbTiN film, and to a film deposited on a substrate having a static permittivity equal to ten.

The important conclusion that can be drawn from the computations described above, is that a large enhancement of the pressure variation ΔP can be achieved by replacing the thin Al plates used in the experiment [31], by a system composed by a thick Au mirror and a NbTiN film having a thickness larger than two hundred nm. To get a quantitative idea of the magnitude of the enhancement that can be achieved in this way, consider as an example a setup with a width $a = 100$ nm, at a temperature $T = 0.5\,T_c$. For the Al system of Ref. [31], one gets $\Delta P = -0.023$ mPa while for the Au-NbTiN setup [with $\mathrm{RRR}_{\mathrm{Au}} = 1$ and $\mathrm{RRR}_{\mathrm{NbTiN}} = 1.12$] one finds $\Delta P = -0.36$ mPa. While this figure represents a 15.8-fold enhancement with respect to the Al system, it is still 16.5 times smaller than the sensitivity of 6 mPa. One can get closer to the sensitivity threshold by decreasing the separation a. For example, going down to $a = 60$ nm, one gets $\Delta P = -0.77$ mPa, which is 7.8 times smaller than the sensitivity. The remaining gap can be partly filled by improving the mean free path ℓ of the Au mirror. If Au mirrors with $\mathrm{RRR} = 3$ can be made, that would give $\Delta P = -0.98$, which is just 6.1 times smaller than the sensitivity. This shows that the effect of the transition would be observable with the Au-NbTiN setup if the sensitivity of the apparatus could be improved by only one order of magnitude.

As a final remark, we note that in the unpublished experiment using a superconducting Au-NbTiN sphere-plate system [30], the Casimir pressure was computed using the Casimir-Gorter two-fluid model Eq. (9) for the permittivity of the superconductor. Unfortunately, the results obtained in this way are not quite correct. Using this model, the authors estimated that for $a = 100$ nm, the variation of the Casimir pressure $\Delta P(a;T)$ for $T \ll T_c$ was of -265 mPa, corresponding to a 5.1% fractional change $\Delta P(T)/P(T_c)$ of the Casimir pressure. The corresponding variation $\Delta P(a;T)$ obtained by us using the BCS permittivity is of -0.42 mPa (see Fig. 6), which amounts to a pressure fractional change $\Delta P(T)/P(T_c) = 8 \times 10^{-5}$. We thus see that the two-fluid model overestimates the magnitude of the pressure variation by a factor larger than 600. We note also that the prediction of a 5.1% change in the pressure is in disagreement with the experimental bound of 2.5%, while of course the prediction of the BCS model is consistent with it.

IV. CONCLUSIONS

A much debated problem in the theory of the Casimir effect is the role of relaxation phenomena of free charge carriers in Lifshitz theory [5,6]. Different prescriptions have been proposed in the literature to compute the Casimir force between conducting test bodies, that go by the names of Drude and plasma prescriptions [5,6]. Superconductors offer a unique possibility to investigate this problem [24]. Unfortunately, it is very difficult to probe the influence of the superconducting transition on the Casimir force, because the effect of the transition is expected to be very small [24]. A recent experiment with thin superconducting Al films reported a null result [31].

In this paper we have developed a detailed theory for the Casimir effect with superconducting plates. Our analysis relies on the Mattis-Bardeen formula for the frequency-dependent conductivity of BCS superconductors, which represents the best known theoretical description of the optical properties of superconductors. We performed numerical computations for Al and for NbTiN, which are the superconductors used in the experiments [31] and [30], respectively. The excellent agreement with the Mattis-Bardeen formula demonstrated by recent optical measurements on superconducting NbTiN [34], lends strong support to the validity of our theoretical analysis. We estimate that for the Al system used in the experiment [31], the magnitude of the variation of the Casimir pressure across the transition is over 250 times smaller than the sensitivity of the experiment. This result, while consistent with the observed null result, makes it unlikely that the effect of the superconducting transition can be observed with an Al setup. We find however that the expected signal can be enhanced by a factor of fifteen by substituting the thin Al films used in Ref. [31] with a Casimir system constituted by a Au mirror and a NbTiN superconducting film, having a thickness larger than 200 nm. The enhancement factor increases to 34 times, if the separation between the plates is decreased from 100 nm to 60 nm. According to our computations, a further improvement is possible by using a Au mirror with a long mean free path for the electrons. Our analysis shows that the effect of the transition to superconductivity would be observable with the Au-NbTiN system, if the sensitivity of the apparatus used in Ref. [31] could be increased by one order of magnitude.

ACKNOWLEDGMENT

The author thanks R. A. Norte for useful discussions on the experiment [31].

APPENDIX: EXPRESSION OF THE FUNCTION $g(\xi)$

In this Appendix we display the explicit expression of the function $g(\xi)$ that enters in Eq. (6), providing the analytic continuation to the imaginary frequency axis of the Mattis-Bardeen formula for the conductivity of a superconductor. Details on its derivation can be found in Ref. [37]. The

function $g(\xi)$ can be expressed as:

$$g(\xi) = \Theta(T_c - T) \int_{-\infty}^{\infty} \frac{d\epsilon}{E} \tanh\left(\frac{E}{2k_B T}\right) \mathrm{Re}[G_+(i\xi, \epsilon)], \tag{A1}$$

where $\Theta(x)$ is the Heaviside step function: $\Theta(x) = 1$ for $x > 0$, and $\Theta(x) = 0$ for $x \leqslant 0$ and

$$G_+(z, \epsilon) = \frac{\epsilon^2 Q_+(z, E) + [Q_+(z, E) + i\hbar\gamma]A_+(z, E)}{Q_+(z, E)\{\epsilon^2 - [Q_+(z, E) + i\hbar\gamma]^2\}}, \tag{A2}$$

with

$$E = \sqrt{\epsilon^2 + \Delta^2}, \tag{A3}$$

$$Q_+(z, E) = \sqrt{(E + \hbar z)^2 - \Delta^2}, \tag{A4}$$

and

$$A_+(z, E) = E(E + \hbar z) + \Delta^2. \tag{A5}$$

Here, Δ is the temperature-dependent gap. From BCS theory [33] one knows that

$$\Delta = c_1 k_B T_c \sqrt{1 - \frac{T}{T_c}} \left(c_2 + c_3 \frac{T}{T_c}\right), \tag{A6}$$

where $c_1 = 1.764$, $c_2 = 0.9963$, and $c_3 = 0.7735$.

[1] H. B. G. Casimir, Proc. K. Ned. Akad. Wet. **51**, 793 (1948).
[2] E. M. Lifshitz, Zh. Eksp. Teor. Fiz. **29**, 94 (1955) [Sov. Phys. JETP **2**, 73 (1956)].
[3] K. A. Milton, *The Casimir Effect: Physical manifestations of Zero-Point Energy* (World Scientific, Singapore, 2001).
[4] V. A. Parsegian, *Van der Waals Forces* (Cambridge University Press, Cambridge, 2005).
[5] M. Bordag, G. L. Klimchitskaya, U. Mohideen, and V. M. Mostepanenko, *Advances in the Casimir Effect* (Oxford University Press, Oxford, 2009).
[6] G. L. Klimchitskaya, U. Mohideen, and V. M. Mostepanenko, Rev. Mod. Phys. **81**, 1827 (2009).
[7] A. W. Rodrigues, F. Capasso, and S. G. Johnson, Nat. Photon. **5**, 211 (2011).
[8] S. Y. Buhmann, *Dispersion Forces I: Macroscopic Quantum Electrodynamics and Ground-State Casimir, Casimir-Polder, and van der Waals Forces* (Springer, Berlin, 2012).
[9] L. M. Woods, D. A. R. Dalvit, A. Tkatchenko, P. Rodriguez-Lopez, A. W. Rodriguez, and R. Podgornik, Rev. Mod. Phys. **88**, 045003 (2016).
[10] G. Bimonte, T. Emig, M. Kardar, and M. Krüger, Ann. Rev. Cond. Matt. Phys. **8**, 119 (2017).
[11] F. Chen, G. L. Klimchitskaya, V. M. Mostepanenko, and U. Mohideen, Phys. Rev. Lett. **97**, 170402 (2006).
[12] F. Chen, U. Mohideen, G. L. Klimchitskaya, and V. M. Mostepanenko, Phys. Rev. A **74**, 022103 (2006).
[13] F. Chen, G. L. Klimchitskaya, V. M. Mostepanenko, and U. Mohideen, Phys. Rev. B **76**, 035338 (2007).
[14] S. de Man, K. Heeck, R. J. Wijngaarden, and D. Iannuzzi, Phys. Rev. Lett. **103**, 040402 (2009).
[15] C.-C. Chang, A. A. Banishev, G. L. Klimchitskaya, V. M. Mostepanenko, and U. Mohideen, Phys. Rev. Lett. **107**, 090403 (2011).
[16] A. A. Banishev, C.-C. Chang, R. Castillo-Garza, G. L. Klimchitskaya, V. M. Mostepanenko, and U. Mohideen, Phys. Rev. B **85**, 045436 (2012).
[17] A. A. Banishev, G. L. Klimchitskaya, V. M. Mostepanenko, and U. Mohideen, Phys. Rev. Lett. **110**, 137401 (2013); Phys. Rev. B **88**, 155410 (2013).
[18] G. Bimonte, D. López, and R. S. Decca, Phys. Rev. B **93**, 184434 (2016).
[19] D. A. T. Somers, J. L. Garrett, K. J. Palm, and J. N. Munday, Nature (London) **564**, 386 (2018).
[20] J. N. Munday, F. Capasso, and V. A. Parsegian, Nature (London) **457**, 170 (2009).
[21] A. Le Cunuder, A. Petrosyan, G. Palasantzas, V. Svetovoy, and S. Ciliberto, Phys. Rev. B **98**, 201408(R) (2018).
[22] G. Bimonte, E. Calloni, G. Esposito, L. Milano, and L. Rosa, Phys. Rev. Lett. **94**, 180402 (2005).
[23] G. Bimonte, E. Calloni, G. Esposito, and L. Rosa, Nucl. Phys. B **726**, 441 (2005).
[24] G. Bimonte, Phys. Rev. A **78**, 062101 (2008).
[25] G. Bimonte, D. Born, E. Calloni, G. Esposito, U. Huebner, E. Il'Ichev, L. Rosa, F. Tafuri, and R. Vaglio, J. Phys. A **41**, 164023 (2008).
[26] A. Allocca, G. Bimonte, D. Born, E. Calloni, G. Esposito, U. Huebner, E. Il'ichev, L. Rosa, and F. Tafuri, J. Supercond. Novel Magn. **25**, 2557 (2012).
[27] G. Bimonte, J. Phys. A **27**, 214021 (2015).
[28] G. Bimonte, Phys. Rev. Lett. **112**, 240401 (2014).
[29] G. Bimonte, Phys. Rev. Lett. **113**, 240405 (2014).
[30] H. J. Eerckens, Ph.D. thesis, Leiden University, 2017.
[31] R. A. Norte, M. Forsch, A. Wallucks, I. Marinković, and S. Gröblacher, Phys. Rev. Lett. **121**, 030405 (2018).
[32] D. C. Mattis and J. Bardeen, Phys. Rev. **111**, 412 (1958).
[33] M. Tinkham, *Introduction to Superconductivity* (McGraw-Hill, New York, 1996).
[34] T. Hong, K. Choi, K. Ik Sim, T. Ha, B. Cheol Park, H. Yamamori, and J. Hoon Kim, J. Appl. Phys. **114**, 243905 (2013).
[35] *Handbook of Optical Constants of Solids*, edited by E. D. Palik (Academic, New York, 1985).
[36] C. J. Gorter and H. Casimir, Physica **1**, 306 (1934).
[37] G. Bimonte, H. Haakh, C. Henkel, and F. Intravaia, J. Phys. A **43**, 145304 (2010).